Mechanical considerations of the continuum for rigid bodies and fluid-structure interactions

K.Chandana, IMMIDISETTY SATYA,KALLEMPUDI VAHINI

Assistent.prof
Department: Mechanical
Visakha Institute of Engineering & Technology,
Division,GVMC,Narava, Visakhapatham, Andhra Pradesh.

Abstract

Continuum mechanical issues for both deformable and rigid solids, as well as fluids, are discussed in this study. All systems are approximated using the same finite element method. Particularly, we provide a standard displacement-based formulation for the deformable solids and use this framework to describe the transformation of the solid into a rigid body in the limit of infinite stiffness. Last but not least, we show how to immerse a discretized solid into a fluid for fluid-structure interaction issues.

Introduction

Oftentimes, a mechanical system may be thought of as a continuum, regardless of how its parts are physically interpreted (see Malvern [12]). Both the Eulerian and Lagrangian descriptions of the local balance of momentum are possible within this continuum mechanical framework. Due to the lack of a universal analytical solution for the considered initial boundary value issue, we use a space-time finite element solution approach to approximate and solve the weak form of the problem (see Hughes [10] for more details). Since the employed degrees of freedom are no longer independent when bodies are assumed to be stiff, a numerical solution cannot be attained inside the typical finite element framework. The finite element system may be rewritten in terms of a skew coordinate system based on a special Caserta theory (see Rubin [13] for details).

By include the rigidity assumptions inside this reformed system, a set of differential-algebraic equations (DAEs) regulating the motion of the rigid body may be obtained. It will be shown that skew coordinate systems are required due to interpolation problems in the director field. These DAEs are the result of a rotation-free formulation made possible by using the new coordinate system directly; for details, see Bertsch [5]. If we use an appropriate null-space approach (see Bertsch [1]), we may further reduce these DAEs to a minimal set of equations in terms of generalized coordinates, and thereby recover the classical Newton-Euler equations. Finally, we demonstrate how to generate an appropriate Euler-Lagrange mapping when immersing a solid in a fluid using the underlying finite element framework (Liu et al. [11] and Herschet al. [8]). Since the solid is seen as a momentum source field emerging from the fluid, this interpretation holds. Since we don't have to Ramesh the fluid at each stage, this approach is preferable for fluid-structure interaction issues. Similar methods have been used to submerge particles;however, they

rely on the contributions of nodal forces rather than the field equations for the solid (Hu et al. [9]).

Continua

In this part, we quickly summarize the key equations that need to be understood. While fluids are modelled using a Eulerian framework in the real con figuration B R 3, developments involving solids are based on a broad non-linear approach inside a Lagrangian framework defined in its reference configuration B0 R 3. In the first part, we review the fundamental equations for a hyperplastic body that may undergo deformation, and in the second section, we modify this formulation to include the characteristics of a rigid body. Subsection three provides a concise review of fluids.

The Mechanics of Materials Subjected to a Discrete Strain

To begin, let's think about a deformation mapping that changes over time: B0 [0, T] R 3, where [0, T] represents the time range between the beginning and conclusion of the motion. Specifically, = (, t) represents the equivalent mapping of the surface. Please be aware that the limits must.

$$\Gamma_u \cup \Gamma_\sigma = \Gamma \quad \text{and} \quad \Gamma_u \cap \Gamma_\sigma = \emptyset$$

where u represents the Dirichlet boundary and the Neumann boundary. For the present state, write but = t. (B0). For simplicity, we will refer to material locations as X B0, material velocity as = /t, and deformation gradient as F = D. On top of that, we assume the presence of a strain energy function

(C): B0 [0, T] R, where C is the right Cauchy-Green deformation tensor and C = F T F. The formula for the linear momentum is v =, where is the density of the reference configuration and is the velocity. This leads to the following Lagrangian expression for the linear momentum conservation:

$$\begin{bmatrix} \dot{\varphi} = \rho_0^{-1}\pi \\ \dot{\pi} = Div(\boldsymbol{P}) + \bar{\boldsymbol{B}} \end{bmatrix}$$

enhanced by the boundary conditions

$$\begin{aligned} \boldsymbol{\varphi} &= \bar{\boldsymbol{\varphi}} \quad \text{on} \quad \Gamma_{\boldsymbol{u}} \times [0,T] \\ \boldsymbol{PN} &= \bar{\boldsymbol{T}} \quad \text{on} \quad \Gamma_{\boldsymbol{\sigma}} \times [0,T] \end{aligned}$$

The first Piola-Kirchhoff stress tensor is denoted by P = 2FC(C), the external tractions at the Neumann boundary are denoted by T, and a body force is denoted by B. More so, the material time derivative is shown as a superimposed dot. For the continuation, we will be using the following notation.

$$\int_{\mathcal{B}_0} (\bullet)\cdot(\bullet)dV =: \langle \bullet, \bullet \rangle \quad \text{and} \quad \int_{\Gamma} (\bullet)\cdot(\bullet)dA =: \langle \bullet, \bullet \rangle_{\Gamma}$$

Then write out how a physical being adds value to the digital project:

$$G(\varphi, \delta\varphi) = \underbrace{\langle \rho_R \ddot{\varphi}, \delta\varphi \rangle}_{G^{dyn}} + \underbrace{\langle \boldsymbol{P}, \nabla_X(\delta\varphi) \rangle}_{G^{int}} \underbrace{- \langle \rho_R \bar{\boldsymbol{B}}, \delta\varphi \rangle - \langle \bar{\boldsymbol{T}}, \delta\varphi \rangle_{\Gamma_\sigma}}_{-G^{ext}}$$

By adding a collection of finite elements e E h to the initial state B0 through a spatial discretization technique, we are able to generate a numerical solution to the nonlinear issue at hand.

$$\mathcal{B}_0^h = \bigcup_{\forall e \in \mathbb{E}^h} \mathcal{B}_e^h$$

We present finite dimensional approximations of and using a finite element method that is based on displacements.

$$\boldsymbol{\varphi}^h = \sum_{A \in \omega} N^A \boldsymbol{q}_A, \quad \text{and} \quad \delta\boldsymbol{\varphi}^h = \sum_{B \in \omega} N^B \delta\boldsymbol{q}_B$$

where the global configuration vector q = [q1,node] is the set of nodal values of the configuration mapping at time t, where a = (XA, t), A, B = 1,node. As an added bonus, the global shape functions connected to nodes A are denoted by the notation N A (X): B h R. It is now possible to express the kinetic energy of the discrete system as

$$T = \frac{1}{2}\langle \rho_0 \boldsymbol{v}^h, \boldsymbol{v}^h \rangle$$

Take note that the associated discrete mass matrix has coefficients that read

$$\boldsymbol{M}^{AB} = \langle \rho_R N^A, N^B \rangle \boldsymbol{I}$$

, where I am the identity matrix and R is the square root of three. Following this, we define the discrete deformation gradient and the discrete deformation tensor.

$$\boldsymbol{F}^h = \frac{\partial \boldsymbol{\varphi}^h}{\partial \boldsymbol{X}} = \sum_{A \in \omega} \boldsymbol{q}_A \otimes \nabla N^A(\boldsymbol{X})$$

and

$$\boldsymbol{C}^h = \sum_{A,B \in \omega} \boldsymbol{q}_A \cdot \boldsymbol{q}_B \nabla N^A(\boldsymbol{X}) \otimes \nabla N^B(\boldsymbol{X})$$

The inner potential function is defined as follows, using the previously provided description of the local strain energy density function:

$$V^{int}(\boldsymbol{q}) = \langle \Psi\left(\boldsymbol{C}^h\right), 1 \rangle$$

As a result, we may represent virtual labour in discrete units as

$$G^{int}\left(\boldsymbol{\varphi}^h, \delta\boldsymbol{\varphi}^h\right) = \sum_{A,B \in \omega} \delta\boldsymbol{q}_A \cdot \boldsymbol{q}_B \langle \nabla N^A(\boldsymbol{X}), \boldsymbol{S}\left(\boldsymbol{C}^h\right) \nabla N^B(\boldsymbol{X}) \rangle$$

where S C h = 2∇CΨ (C h) denotes the second Piola-Kirchhoff stress tensoar. Furthermore, we assume the existence of an external potential energy function.

$$V^{ext}(\boldsymbol{q}) = \sum_{A \in \omega} \boldsymbol{q}_A \cdot \left(\langle N^A, \boldsymbol{B} \rangle + \langle N^A, \bar{\boldsymbol{T}} \rangle_{\Gamma_\sigma} \right)$$

in addition, we derive a statement of the external contributions to the virtual labour done in discrete units.

$$G^{ext}\left(\boldsymbol{\varphi}^h, \delta\boldsymbol{\varphi}^h\right) = \delta\boldsymbol{q} \cdot \nabla V^{ext}(\boldsymbol{q})$$

Since it is required that (5) holds true for every given test function, we end up with a universal nonlinear set of equations,

$$\left[\begin{array}{l} \dot{\boldsymbol{q}} = \boldsymbol{v} \\ \boldsymbol{M}\dot{\boldsymbol{v}} = -\left[\nabla V^{\text{int}}(\boldsymbol{q}) - \nabla V^{\text{ext}}(\boldsymbol{q})\right] \end{array}\right]$$

It requires a suitable time stepping technique for resolution. Therefore, we partition the period under consideration into a set of subintervals, nn+1, and get

$$\left[\begin{array}{l} \boldsymbol{q}_{n+1} - \boldsymbol{q}_n = \Delta t \boldsymbol{v}_{n+1/2} \\ \boldsymbol{M}(\boldsymbol{v}_{n+1} - \boldsymbol{v}_n) = -\Delta t\left[\overline{\nabla} V^{\text{int}}(\boldsymbol{q}_{n+1}, \boldsymbol{q}_n) - \nabla V^{\text{ext}}(\boldsymbol{q}_{n+1/2})\right] \end{array}\right]$$

where ∇V int (qn+1,an) represents the discrete gradient in the sense of GonziLez [7]. Note that (17) conserves algorithmically energy and both momentum maps, see Bertsch& Steinmann [3].

Bodies with a rigid structure

After introducing a discrete and deformable system, we now wish to impose enough constraints on it that it does not change shape at all throughout the period of time under consideration. Using the Caserta point theory (see Rubin [13]), we introduce a local coordinate system that is fixed to the reference position of the body at a point X 1 and uses convective coordinates I to determine the location of each point in the mesh.

$$\boldsymbol{\varphi}^{\text{h}} = \sum_{A\in\omega} N^A \boldsymbol{q}_A, \quad \boldsymbol{q}_A(\theta^i, t) = \bar{\boldsymbol{\varphi}}(\bar{\boldsymbol{X}}, t) + \theta^i_A \boldsymbol{d}_i(t)$$

Here, di(t) R 3 is the non-orthogonal director frame at time t, and (X, t) R 3 is the position vector of the reference point at time t. The kinematic foundations of body stiffness are stated as

$$\begin{array}{c} \theta^i \neq \theta^i(t) \\ \boldsymbol{d}_i \cdot \boldsymbol{d}_j - (\boldsymbol{d}_i \cdot \boldsymbol{d}_j)_{\text{ref}} = 0 \end{array}$$

i.e., the convective coordinates θ Iam not a function

n of time and the director triad does not deform. The motion of the rigid body is now characterized only by its kinetic energy and the constraints in (Eq. 19), since no internal stresses appear, i.e., V int(q) = 0, ∀t ∈ [0, T]. Analogues to (Eq. 8), we can now write for the kinetic energy

$$T = \frac{1}{2}\sum_{e\in\mathbb{E}^{\text{h}}} \langle \rho_0 \boldsymbol{v}^{\text{h}}, \boldsymbol{v}^{\text{h}} \rangle^e_\theta$$

utilizing the speed that would be expected given (18)

$$\boldsymbol{v}^{\text{h}} = \sum_{A\in\omega} N^A \boldsymbol{v}_A, \quad \boldsymbol{v}_A(\theta^i, t) = \boldsymbol{v}_\varphi(\bar{\boldsymbol{X}}, t) + \theta^i_A \boldsymbol{v}_i(t)$$

and the elementwise integration

$$\langle \bullet, \bullet \rangle^e_\theta = \int_{\mathcal{B}^{\text{h}}_e} (\bullet)\cdot(\bullet)\det(\boldsymbol{R})\mathrm{d}\boldsymbol{\theta}$$

where R = [d1 d2 d3], R ∈ R 3×3. For convenience, we introduce the extended position vector q¯ = [ϕ¯, d1, d2, d3] T, q¯ ∈ R 12 and obtain the corresponding constant mass matrix of the rigid body by inserting (22) into (21)

$$\bar{\boldsymbol{M}} = \begin{bmatrix} \boldsymbol{M}_\varphi & \boldsymbol{e}^1 & \boldsymbol{e}^2 & \boldsymbol{e}^3 \\ \boldsymbol{e}^1 & \boldsymbol{E}^{11} & \boldsymbol{E}^{12} & \boldsymbol{E}^{13} \\ \boldsymbol{e}^2 & \boldsymbol{E}^{21} & \boldsymbol{E}^{22} & \boldsymbol{E}^{23} \\ \boldsymbol{e}^3 & \boldsymbol{E}^{31} & \boldsymbol{E}^{32} & \boldsymbol{E}^{33} \end{bmatrix}$$

where

$$\boldsymbol{M}_\varphi = \sum_{e\in\mathbb{E}^{\text{h}}} \langle \rho_0, 1\rangle^e_\theta \boldsymbol{I}, \quad \boldsymbol{e}^i = \sum_{e\in\mathbb{E}^{\text{h}}} \langle \rho_0, N^A\theta^i_A\rangle^e_\theta \boldsymbol{I}$$

$$\boldsymbol{E}^{ij} = \sum_{e\in\mathbb{E}^{\text{h}}} \langle \rho_0, N^A N^B \theta^i_A \theta^j_B\rangle^e_\theta \boldsymbol{I}$$

Keep in mind that if (X, t) is placed at the body's center of mass, then e I = 0 and if the directors di are orthonormal and coincide with the primary axis of inertia, then the matrix E will be diagonal. Next, we rewrite the external contributions in terms of the convective coordinates, assuming that the body force B (I t) and the Neumann boundary contributions T (I t) can be expressed in terms of the convective coordinates, as follows:

$$G^{\text{ext}}(\bar{\boldsymbol{q}}, \delta\bar{\boldsymbol{q}}) = \sum_{e\in\mathbb{E}^{\text{h}}} \left(\langle \delta\boldsymbol{\varphi}^{\text{h}}, \bar{\boldsymbol{B}}\rangle^e_\theta + \langle \delta\boldsymbol{\varphi}^{\text{h}}, \bar{\boldsymbol{T}}\rangle^e_{\theta,\Gamma_\sigma} \right)$$

where $\delta\boldsymbol{\varphi}^{\text{h}} = \sum_{A\in\omega} N^A(\delta\boldsymbol{\varphi}(\bar{\boldsymbol{X}}, t) + \theta^i_A \delta\boldsymbol{d}_i(t))$. Rearranging all terms correspond-

ing to the position vector $\bar{\boldsymbol{q}}$ yields

$$G^{\text{ext}}(\bar{\boldsymbol{q}}, \delta\bar{\boldsymbol{q}}) = \delta\bar{\boldsymbol{q}}\cdot\nabla_{\bar{\boldsymbol{q}}} V^{\text{ext}}(\bar{\boldsymbol{q}}) = \delta\bar{\boldsymbol{q}}\cdot\bar{\boldsymbol{F}}, \quad \bar{\boldsymbol{F}} = [f_\varphi, f^1, f^2, f^3]^T$$

where

$$f_{\varphi} = \sum_{e \in \mathbb{E}^h} \left(\langle \bar{\boldsymbol{B}}, 1 \rangle_{\theta}^{e} + \langle \bar{\boldsymbol{T}}, 1 \rangle_{\theta, \Gamma_{\sigma}}^{e} \right)$$

$$f^{i} = \sum_{e \in \mathbb{E}^h} \left(\langle \bar{\boldsymbol{B}}, N^{A} \theta_{A}^{i} \rangle_{\theta}^{e} + \langle \bar{\boldsymbol{T}}, N^{A} \theta_{A}^{i} \rangle_{\theta, \Gamma_{\sigma}}^{e} \right)$$

Keep in mind that the kinematic connection vi = di where R 3 indicates the angular velocity allows us to relate Neumann contributions to the director momentum in terms of an external torque m. This motivates us to determine the external torque's power contributions.

$$\boldsymbol{m} \cdot \boldsymbol{\omega} = \frac{1}{2} \boldsymbol{m} \cdot (\boldsymbol{d}^{i} \times \boldsymbol{v}_{i}) = \frac{1}{2} \boldsymbol{v}_{i} \cdot (\boldsymbol{m} \times \boldsymbol{d}^{i}) = \boldsymbol{v}_{i} \cdot \boldsymbol{f}^{i}$$

and obtain for the external director momentum

$$\boldsymbol{f}^{i} = \frac{1}{2} \boldsymbol{m} \times \boldsymbol{d}^{i}$$

The constant application of external torque (30) was first suggested in Bertsch et al. Finally, we use (20) to calculate the constraint forces, which are expressed as follows:

$$\Phi(\bar{\boldsymbol{q}}) = \frac{1}{2} (\boldsymbol{d}_{i} \cdot \boldsymbol{d}_{j} - (\boldsymbol{d}_{i} \cdot \boldsymbol{d}_{j})_{\mathrm{ref}})$$

as well as collect data on how much of the virtual labour is due to constraints

$$G^{\mathrm{con}}(\bar{\boldsymbol{q}}, \delta\bar{\boldsymbol{q}}) = \delta\bar{\boldsymbol{q}} \cdot \bar{\boldsymbol{F}}^{\mathrm{con}}, \quad \bar{\boldsymbol{F}}^{\mathrm{con}} = [f_{c}, f_{c}^{1}, f_{c}^{2}, f_{c}^{3}]^{T}$$

Since the constraints (31) do not depend on ϕ (X¯, t), f c = 0. The remaining terms are given by

$$f_{c}^{i} = \nabla_{d_{i}} \Phi(\bar{\boldsymbol{q}}) \cdot \boldsymbol{\lambda} = \Lambda^{ij} \boldsymbol{d}_{j}, \quad \left[\lambda^{ij}\right] = \begin{bmatrix} \lambda^{1} & \lambda^{4} & \lambda^{5} \\ \lambda^{4} & \lambda^{2} & \lambda^{6} \\ \lambda^{5} & \lambda^{6} & \lambda^{3} \end{bmatrix}$$

where I am a multiplier of the Lagrange type. A nonlinear set of equations analogous to (16)

$$\begin{bmatrix} \dot{\bar{\boldsymbol{q}}} = \bar{\boldsymbol{v}} \\ \bar{\boldsymbol{M}} \dot{\bar{\boldsymbol{v}}} = -\left[\nabla_{\bar{q}} \Phi(\bar{\boldsymbol{q}}) \cdot \boldsymbol{\lambda} - \nabla_{\bar{q}} V^{\mathrm{ext}}(\bar{\boldsymbol{q}})\right] \\ \Phi(\bar{\boldsymbol{q}}) = \boldsymbol{0} \end{bmatrix}$$

It once again has to be addressed by a method of time stepping that works. This time around, too, we use a rule of thumb based on the midpoint (see Bertsch& Steinmann [4])

$$\begin{bmatrix} \bar{\boldsymbol{q}}_{n+1} - \bar{\boldsymbol{q}}_{n} = \Delta t \bar{\boldsymbol{v}}_{n+1/2} \\ \bar{\boldsymbol{M}}(\bar{\boldsymbol{v}}_{n+1} - \bar{\boldsymbol{v}}_{n}) = -\Delta t \left[\nabla_{\bar{q}} \Phi(\bar{\boldsymbol{q}}_{n+1/2}) \cdot \boldsymbol{\lambda} - \nabla_{\bar{q}} V^{\mathrm{ext}}(\bar{\boldsymbol{q}}_{n+1/2})\right] \\ \Phi(\bar{\boldsymbol{q}}_{n+1}) = \boldsymbol{0} \end{bmatrix}$$

while taking into account the constraints on the system. Several mechanical parameters, including total energy and the components of angular momentum, are algorithmically conserved by the chosen kind of a midpoint rule. It is important to keep in mind that the limitations in (31) are met at time n + 1, and not at time n + 1/2.

Fluids

Here, we propose a finite element formulation of fluids as a first step toward describing the interaction of fluids and structures in the future. This leads us to express the fluid system in terms of a Eulerian description through the inverse mapping X = 1 (x(t), t). It is obvious that f (x(t), t) is the time differential of a physical quantity.

$$\left.\frac{\partial f}{\partial t}\right|_{X} = \left.\frac{\partial f}{\partial t}\right|_{x} + \boldsymbol{v} \cdot \nabla_{x} f$$

We focus on the incompressible situation without sacrificing generality, and derive the continuity condition.

$$\nabla_{x} \cdot \boldsymbol{v} = \frac{1}{J} \dot{J} \equiv 0$$

where J = det(F). For a Newtonian fluid the Cauchy stress tensor σ: B × [0, T] → R d×d is defined by

$$\boldsymbol{\sigma} = -p\boldsymbol{I} + \mu \left(\nabla_{x} \boldsymbol{v} + \nabla_{x} \boldsymbol{v}^{T} \right)$$

In this case, the force exerted by the pressure p: B [0, T] R may be thought of as a Lagrange multiplier (37). Additionally, in this context, stands for dynamic viscosity. The linear momentum balance may be written in the Eulerian form.

$$\rho \dot{\boldsymbol{v}} = \nabla_{x} \cdot \boldsymbol{\sigma} + \rho \boldsymbol{b}$$

where and b represent the actual density and a body force that has been specified for this arrangement. The equation of balance, expressed in its weak form, looks like

$$\langle \rho(\dot{v} - \boldsymbol{b}), \delta v \rangle_{\mathcal{B}} + \langle \sigma, \nabla_{x}(\delta v) \rangle_{\mathcal{B}} - \langle \boldsymbol{t}, \delta v \rangle_{\gamma_{\sigma}} = 0$$

added to the limitations

$$\langle \nabla_x \cdot \boldsymbol{v}, \delta p \rangle_{\mathcal{B}} = 0$$

By applying the Lagrange multiplier field analogy to (Eq. 7) and using a conventional Galperin based discretization of the velocity, we get the semi-discrete balance of momentum.

$$\langle \rho^f (\dot{\boldsymbol{v}}^h - \boldsymbol{b}^h), \delta \boldsymbol{v}^h \rangle_{\mathcal{B}} + \langle \boldsymbol{\sigma}^f (\boldsymbol{v}^h, p^h), \nabla_x (\delta \boldsymbol{v}^h) \rangle_{\mathcal{B}} - \langle \boldsymbol{t}^h, \delta \boldsymbol{v}^h \rangle_{\gamma^\sigma} = 0$$

together with the semi-discrete incompressibility criterion

$$\langle \nabla_x \cdot \boldsymbol{v}^h, \delta p^h \rangle_{\mathcal{B}} = 0$$

A stabilization mechanism for the underlying Galperin approach may be used if required (e.g., for low order elements or high Reynolds numbers) (cf. Tezpur [14]) with the help of Enhanced Spaces for Testing Functions

$$\mathbb{V}^{\tilde{v}} =: \{\delta \tilde{\boldsymbol{v}} \in \mathbb{H}^1(\Omega) | \ \delta \tilde{\boldsymbol{v}} = \delta \boldsymbol{v} + \gamma_{\text{SUPG}} \boldsymbol{v} \cdot \nabla_x (\delta \boldsymbol{v}) + \gamma_{\text{PSPG}} \nabla_x (\delta p)\}$$

$$\mathbb{V}^{\tilde{p}} =: \{\delta \tilde{p} \in L_2(\Omega) | \ \delta \tilde{p} = \delta p + \gamma_{\text{LSIC}} \nabla_x \cdot (\delta \boldsymbol{v})\}$$

where SUPG, PSPG, and LSIC are stabilizer parameters determined beforehand. The updated semi-discrete linear momentum balancing formula is as follows:

$$\langle \rho^f (\dot{\boldsymbol{v}}^h - \boldsymbol{b}^h), \delta \boldsymbol{v}^h \rangle_{\mathcal{B}} + \langle \boldsymbol{\sigma}^f (\boldsymbol{v}^h, p^h), \nabla_x (\delta \boldsymbol{v}^h) \rangle_{\mathcal{B}} - \langle \boldsymbol{t}^h, \delta \boldsymbol{v}^h \rangle_{\gamma^\sigma} + \sum_e \gamma_{\text{SUPG}} \langle \mathcal{R}_v, (\boldsymbol{v}^h \cdot \nabla_x) \delta \boldsymbol{v}^h \rangle_{\mathcal{B}} + \sum_e \gamma_{\text{LSIC}} \langle \mathcal{R}_p, \nabla_x \cdot \delta \boldsymbol{v}^h \rangle_{\mathcal{B}} = 0$$

and the kinematic constraint

$$\langle \nabla_x \cdot \boldsymbol{v}^h, \delta p^h \rangle + \sum_e \gamma_{\text{PSPG}} \langle \mathcal{R}_v, \nabla_x \delta \boldsymbol{p}^h \rangle_{\mathcal{B}} = 0$$

The initial momentum residuals Rv and the kinematic constraint residuals Rp are the quantities of interest here. It is possible to make a temporal discretization of equations (42) and (43) by using the midpoint type rule discussed before.

$$\left\langle \rho \left(\frac{\boldsymbol{v}_{n+1}^h - \boldsymbol{v}_n^h}{\Delta t} - (\boldsymbol{v}_{n+1/2}{}^h \cdot \nabla_x) \boldsymbol{v}_{n+1/2}^h - \boldsymbol{g}_{n+1/2}^h \right), \delta \boldsymbol{v}^h \right\rangle +$$
$$\langle \boldsymbol{\sigma}(\boldsymbol{v}_{n+1/2}^h, p_{n+1}^h), \nabla_x (\delta \boldsymbol{v}^h) \rangle - \langle \boldsymbol{h}_{n+1/2}^h, \delta \boldsymbol{v}^h \rangle_{\Gamma^h} = 0$$
$$\langle \nabla_x \cdot \boldsymbol{v}_{n+1}^h, \delta p^h \rangle = 0$$

The completely discrete stabilized version is provided in full in Hersch et al. [8], so it's easy to see where this is going.

Interaction between fluid and structure

Whenever we need to determine how a fluid will react to a solid, we do it by completely submerging the solid system in the fluid under (see Liu et al. [15]). Here we reformulate (Eq. 39) to include the resultant forces of the solid system, located in the domain B s t at time t as volumetric force F: B s t [0, T] R 3 into the fluid's linear momentum balance. 2

$$\rho^f \dot{\boldsymbol{v}} = \nabla_x \cdot \boldsymbol{\sigma}^f + \rho^f \boldsymbol{b} + \boldsymbol{\mathcal{F}}$$

The force field of the immersed solid reads

$$\boldsymbol{\mathcal{F}} = \begin{cases} \boldsymbol{0} & \text{in} \quad \mathcal{B} \backslash \mathcal{B}^s \\ (\rho^f - \rho^s)(\dot{\boldsymbol{v}} - \boldsymbol{b}) + \nabla \cdot (\boldsymbol{\sigma}^s - \boldsymbol{\sigma}^f) & \text{in} \quad \mathcal{B}^s \end{cases}$$

Pushing forward the purely material derivative of the strain energy function allows us to derive the solid's true stress field.

$$\boldsymbol{\sigma}^s = \frac{2}{J} \boldsymbol{F} \cdot \frac{\partial \Psi(\boldsymbol{C})}{\partial \boldsymbol{C}} \boldsymbol{F}^T$$

Lagrangian mapping is used for the submerged solid because of its physical qualities, whereas Eulerian mapping is used for the fluid. For each function of the solid system, we need to define a Euler-Lagrange mapping IB s t in the space B s t B such that (x, t) translates to IB s t ((X, t)): B s 0 [0, T]. In part because of this, we've decided to chart

$$\boldsymbol{v}(\boldsymbol{x}(t), t) = \mathcal{I}_{\mathcal{B}_t^s}(\boldsymbol{v}(\boldsymbol{X}, t))$$

We finish up the system of equations by defining proper Dirichlet boundary conditions for the submerged solid.

$$\boldsymbol{x}(\boldsymbol{X}, t) = \tilde{\boldsymbol{x}}, \quad \text{on} \quad \partial \mathcal{B}_D^s$$

Because the solid is enveloped by the fluid, extra Neumann boundary conditions are not explicitly considered. As

a result, the equivalent weak form is as follows:

$$\langle \rho^f(\dot{v} - b) - \mathcal{F}, \delta v \rangle_{\mathcal{B}} + \langle \sigma^f, \nabla_x(\delta v) \rangle_{\mathcal{B}} - \langle t, \delta v \rangle_{\gamma^h} = 0$$

and for the constraints

$$\langle \nabla_x \cdot v, \delta p \rangle_{\mathcal{B}} = 0$$

Similar to (45), we consider the spatial discretization of the fluid and instead concentrate on the discretization of the volumetric force field of the submerged solid.

$$\begin{aligned} \mathcal{F}^h(v,p) = & \langle (\rho_0^f - \rho_0^s)\left(\mathcal{I}_{\mathcal{B}_t^s}(v^h) - b^h\right), \mathcal{I}_{\mathcal{B}_t^s}(\delta \tilde{v}^h) \rangle_{\mathcal{B}_0}^s \\ & - \langle S^s, (F^s(\mathcal{I}_{\mathcal{B}_t^s}(v^h)))^T \nabla_X \mathcal{I}_{\mathcal{B}_t^s}(\delta \tilde{v}^h) \rangle_{\mathcal{B}_0}^s \\ & + \langle \tilde{\sigma}^f(\mathcal{I}_{\mathcal{B}_t^s}(v^h), \mathcal{I}_{\mathcal{B}_t^s}(p^h)), \nabla_x \mathcal{I}_{\mathcal{B}_t^s}(\delta \tilde{v}^h) J^s(\mathcal{I}_{\mathcal{B}_t^s}(v^h)) \rangle_{\mathcal{B}_0}^s \end{aligned}$$

where we use an IFEM approach for the Euler-Lagrange mapping

$$\mathcal{I}_{\mathcal{B}_t^s}(N^A(X,t)) = \sum_{C=1}^{n_{\text{node}}} N^A(x(X_C,t))\bar{N}_C(X)$$

See Hersch et al. [8] for an easy-to-follow explanation of the time-consuming but worthwhile process of discretization.

Real-World Illustration with Numbers

In this case we see how submerged approaches may be used to solve bivascular issues in an automobile. As a result, we think of blood as being incompressible. With a density of 1105 and a viscosity of 1, a new toning fluid is very viscous. To the left of the channel, a Poiseuille inflow is applied with the amplitude function A(t) = 5 (sin(2t) + 1.1), whereas the right-hand side of the channel has no boundary conditions put on it (see Fig. 1). With the Lame' parameters s = 8 106 and s = 2 106, the flaps are represented as Neo-Hookean solids with a Young's modulus of E = 5.6 106 and a Poisson ratio of v = 0.4. As the space between the two flaps represents insufficiency in a human heart valve, you may think of them as a model (cf. Gil et al. [6]

.

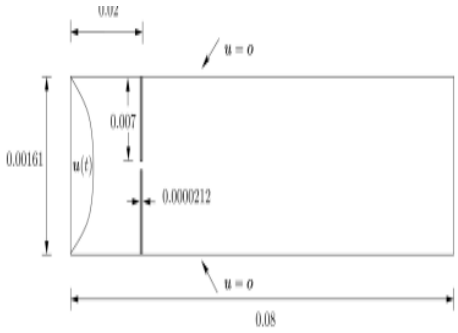

Figure 1: The geometry and boundary conditions for two fluttering membranes.

Using 256x64 Q1Q1 fluid and 40x4 bilinear solid components, Fig. 2 depicts the temporal development of the pulsatile flow.

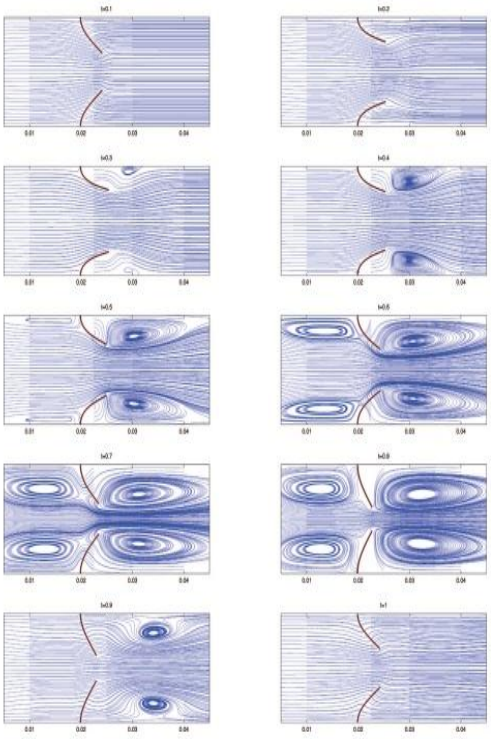

Fluid membranes and streamlines with time (Fig.2)

the X and Y movement of the top leaflet tip for various discretization's. If the mesh size is small enough, the Q1Q1 fluid finite element discretization yields the same results as the Q2Q1 discretization. The converged findings correspond exactly with those produced by Gil et AL Immersed.'s Structural Potential Method (ISPM) in their paper [6]. Hersch et al. [8] provide a comprehensive comparison of these various submersion methods.

Conclusions

For the first time, we have introduced a non-linear framework for deformable bodies based on a generic

continuum mechanical description. Just a moment

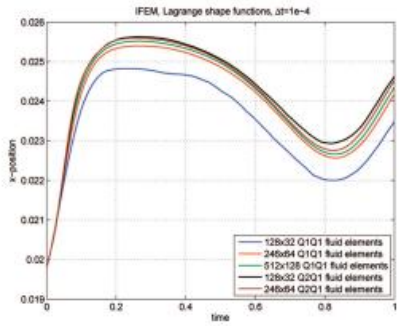

Fig. 3. X-Position of the tip of the upper leaflet

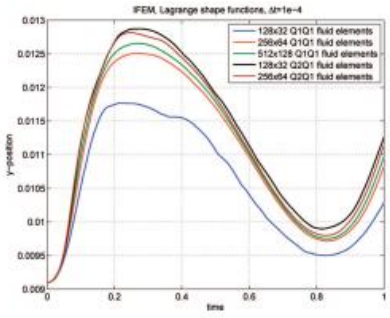

Figure 4: The Y-position of the top leaflet's tip in the limit of infinite stiffness, a new, more general method has been developed to reformulate the discretized body as a restricted system with a redundantdent set of coordinates. Rigid body coordinates are not constrained in any way, allowing for the use of non-equidistant or otherwise non-standard coordinate systems.

This is crucial because it allows us to correct for the directors' interpolation problems, for instance by using a mid-point type rule for the discretization in time. Our work culminates in a demonstration of how to fully submerge a system into a fluid, with the solid being treated as a momentum source field in the fluid. This future study will extend the rigid body assumptions to the immersed system, allowing for a simple and direct treatment of rigid bodies in fluids. This page lays the groundwork for the rest of the project.

REFERENCES

[1] P. Bertsch: The discrete null space method for the energy consistent integration of constrained mechanical systems Part I: Holonomic constraints. Compute. Methods Appl. Mech. Engg., 194:5159–5190, 2005.

[2] P. Bertsch, R. Siebert, N. Sanger: Natural coordinates in the optimal control of multibody systems Sie. J. Compute. Nonlinear Dynam., 7(1):011009/1-8, 2011.

[3] P. Bets Chand, P. Steinmann: Conserving properties of a time FE method – Part II: Timestepping schemes for non-linear electrodynamics. Int. J. Number. Methods Eng., 50:1931–1955, 2001.

[4] P. Bets Chand, P. Steinmann: Conservation Properties of a Time FE Method. Part III: Mechemical systems with holonomic constraints. Int. J. Number. Methods Eng., 53:2271–2304, 2002.

[5] P. Bets Chand, S. Uhlar: Energy-momentum conserving integration of multibody dynamics. Multibody System Dynamics, 17(4):243–289, 2007.

[6] A.J. Gil, A. Arranz Carreon, J. Bonet, O. Hassan: The immersed structural potential method ˜ for haemodynamic applications. Journal of Computational Physics, 229:8613–8641, 2010.

[7] O. Gonzalez: Time integration and discrete Hamiltonian systems. J. Nonlinear Sci., 6:449–467, 1996.

[8] C. Hersch, A.J. Gil, A. Arranz Carreon, J. Bonet: On immersed techniques for fluid-structure ˜ interaction. Compute. Methods Appl. Mech. Engrg., 247–248:51–64, 2012.

[9] H.H. Hu, N.A. Patankar, M.Y. Zhu: Direct numerical simulations of fluid-soli systems using the arbitrary Lagrangian-Eulerian technique. Journal of Computational Physics, 169:427–462, 2001.

[10] T.J.R. Hughes: The Finite Element Method. Dover Publications, 2000.

[11] W.K. Liu, D.W. Kim, S. Tang: Mathematical foundations of the immersed finite lement method. Computational Mechanics, 39:211–222, 2007.

[12] L.E. Malvern: Introduction to the mechanics of a continuous medium. Prentice Hall, 1969.

[13] M.B. Rubin: Caserta Theories: Shells, Rods and Points. Kluwer Academic Publishers, 2010.

[14] T.E. Tezpur: Stabilized finite element for mutations for incompressible flow computations. Advances in applied mechanics, 28:1–44, 1992.

[15] L. Zhang, A. Grettenberger, X. Wang, W.K. Liu: Immersed finite element method. Compute. Methods Appl. Mech. Engg., 193:2051–2067, 2004.